



ACCOUNTING FOR METEOROLOGICAL EFFECTS IN THE DETECTOR OF THE CHARGED COMPONENT OF COSMIC RAYS

Maxim Philippov¹, Vladimir Makhmutov¹, Galina Bazilevskaya¹, Fedor
Zagumennov^{2,3}, Vladimir Fomenko², Yuri Stozhkov¹, Andrey Orlov¹

5 ¹P. N. Lebedev Physical Institute of the Russian Academy of Sciences, Moscow, Russian
Federation

²Federal State Budgetary Institution «Central Aerological Observatory», Dolgoprudny, Russian
Federation

³Plekhanov Russian University of Economics, Moscow, Russian Federation

10 *Correspondence to:* Maxim Philippov (mfilippov@frtk.ru)

Abstract. In this paper, we discuss the influence of meteorological effects on the data of the
ground installation CARPET, which is a detector of the charged component of secondary cosmic
rays (CRs). This device is designed in the P.N. Lebedev Physical Institute (LPI, Moscow, Russia)
and installed at the Dolgoprudny scientific station (Dolgoprudny, Moscow region, 55.56 °,
15 W37.3 °; $R_c = 2.12$ GV) in 2017. Based on the data obtained in 2019–2020, the barometric and
temperature coefficients for the CARPET installation were determined. The barometric coefficient
was calculated from the data of the barometric pressure sensor included in the installation. To
determine the temperature effect, we used the data of upper-air sounding of the atmosphere
obtained by the Federal State Budgetary Institution «Central Aerological Observatory» (CAO),
20 also located in Dolgoprudny.

Keywords: cosmic rays; CARPET detector; meteorological effects

1. Introduction

The CARPET installation is designed for permanent monitoring of charged component of
secondary CRs flux at the ground level. It allows analysis of secondary CRs fluxes variations,
25 caused by geomagnetic and solar activity on the processes affecting the behavior of cosmic rays in
near-Earth space and Earth's atmosphere (Makhmutov et al., 2013, 2015).

The basis of the CARPET installation (Fig. 1) is the STS-6 gas-discharge Geiger – Müller counters,
combined in 12 detector blocks of 10 counters each. The detector block consists of two layers: 5
upper and 5 lower counters, separated with an aluminum absorber (filter) 7 mm thick. Experimental
30 data are recorded using three channels with a time resolution of 1 ms. The first channel (UP)
corresponds to the integral count rate of charged particles passing through the top layer of 60
counters. The second channel (LOW) corresponds to the integral count of charged particles passing



through the bottom layer of 60 counters. Particles simultaneously registered by any of the upper and lower counters, i.e., passed through the filter are registered in the coincidence channel - TEL.

35 In addition, there is a channel of auxiliary information ("telemetry"), which consist of the data on pressure, temperature and supply voltages.

The CARPET installation detects particles of the following energies: in the UP and the LOW channels there are electrons and positrons with energies $E > 200$ keV, protons with $E > 5$ MeV, muons with $E > 1.5$ MeV, and photons with $E > 20$ keV (efficiency $< 1\%$). The TEL coincidence
 40 channel registers more energetic particles: electrons with energies $E > 5$ MeV, protons with $E > 30$ MeV, and muons with $E > 15.5$ MeV. Detailed information on the principles of CARPET operation was given previously (Philippov et al., 2020a).

Nowdays there is an international network of the CARPET installations: first module was launched in 2006 (De Mendonca et al., 2011, 2013; Mizin et al., 2011) at CASLEO (San Juan, Argentina,
 45 $S31.47^\circ$, $W69.17^\circ$, $R_c = 9.8$ GV), two modules were launched (Maghrabi et al., 2020) in 2015 at KACST (King Abdulaziz City for Science and Technology, Saudi Arabia, Riyadh, $S24.39^\circ$, $E46.42^\circ$; $R_c = 14.4$ GV). In 2015 and 2016 at L.N. Gumilyov Eurasian National University (Nur-Sultan, Republic of Kazakhstan, $S51.10^\circ$, $W71.26^\circ$; $R_c = 2.9$ GV), the first and second modules of the CARPET installation were launched (Philippov et al., 2020b; Tulekov et al., 2020).

50 This paper investigates the influence of meteorological conditions on the data of the installation, which has been operating since 2017 at the Dolgoprudny Scientific Station of the Lebedev Physical Institute RAS.

2. Instrumentation and data analysis

2.1 Barometric effect

55 Ground-based CARPET installations detect secondary charged particles, mainly muons, generated in the interaction of primary CRs with nuclei in the atmosphere. Muons are not nuclear-active particles and lose energy for the excitation and ionization of air atoms; therefore, it is necessary to take into account the barometric and temperature effects (Dorman, 1972, 2004, 2006).

The barometric effect can be determined through variations in atmospheric pressure at the level of
 60 CRs registration (equation 1):

$$\left(\frac{\Delta N}{N_0}\right)_P \cong \beta \Delta P, \quad (1)$$

where

$\left(\frac{\Delta N}{N_0}\right)_P$ – relative variation of the count rate of the CARPET installation;



$$\Delta N = N - N_0;$$

$$\Delta P = P - P_0;$$

65 N_0 – average (standard) count rate [pulses/h] for the period of measurements;

N – current count rate [pulses/h];

P_0 – average (standard) ground atmospheric pressure [hPa] for the period of measurements;

P – current atmospheric pressure [hPa].

According to the data for 2019, hourly averaged average count rate and atmospheric pressure for
 70 the CARPET-MOSCOW installation $N_0 = 53667$ pulses/h, $\sigma_N = 2187$ pulses/h; $P_0 = 988.7$ hPa, $\sigma_P = 9.8$ hPa.

For calculating the barometric coefficient β , it is necessary to determine the linear relationship
 between $\frac{\Delta N}{N_0}$ and ΔP (Fig. 2). Barometric coefficient β for the CARPET-MOSCOW installation is
 determined on the data of June 2019 (During this period there were no significant geomagnetic
 75 and solar disturbances): $\beta = -0.1861 \pm 0.0025\%/hPa$; coefficient of determination $R^2 = 0.8975$.
 Using Eq. (1), we obtain pressure-corrected data:

$$N_{PC} = N - \beta N_0 \Delta P, \quad (2)$$

where

N_{PC} – pressure corrected count rate [impulses/h] of the CARPET installation.

To estimate primary CRs variations, we use pressure corrected data of the Moscow neutron
 80 monitor (<http://cr0.izmiran.ru/mosc/>). Average count rate according to the data of 2019: $\overline{N_{nm}} = 9699$ pulses/min; $\sigma_{nm} = 66$ pulses/min.

Fig. 3 shows neutron monitor count rate variations on the data of 2019. Black horizontal line is
 average count rate [pulses/min]. Upper horizontal data series is standard deviation from the
 average count rate for each month. The relative magnitude of the effect determined by the
 85 variations in primary CRs over a given period of time can be estimated by the ratio $\sigma_{nm}/\overline{N_{nm}} = 0.007$ (0,7%).

Magnitude of the barometric effect of the CARPET-MOSCOW can be estimated as
 $\beta\sigma_P = 0.018$ (1.8%), which is more than 2 times higher than variations of primary CRs. Therefore,
 the barometric effect is significant for the CARPET installations and must be taken into account
 90 in the further data processing.

2.2 Temperature effect

The muon component of secondary CRs is characterized by a significant temperature effect
 (Yanke, et al., 2011), to eliminate which it is necessary to carry out upper-air sounding near the
 instrument. The temperature effect has two components: negative and positive. The negative



95 temperature effect is associated with a decrease in muon fluxes during heating and expansion of
 the atmosphere. The positive temperature effect is associated with the appearance of additional
 muons, as a result of an increase in the rate of decays of charged pions (Dorman, 1972, 2004, 2006;
 Yanke et al., 2011).

To estimate the temperature effect, we used data of the TEL channel of the CARPET – MOSCOW
 100 installation for 2019–2020. The altitude profiles of temperature and pressure were determined
 from the experimental data of the Central Aerological Observatory (CAO; Dolgoprudny).

The temperature effect was determined in two ways: based on the effective generation level
 method and the integral method (Dmitrieva et al., 2013; Ganeva et al., 2013; Zazyan et al., 2015).

2.2.1 Effective generation level method

105 To eliminate the barometric effect, original data (Fig. 4a) were processed according to Equation 1
 (Fig. 4b). The barometric correction mainly compensates for the daily variations in the count rate.
 The effective generation rate method is based on the assumption that muons are mainly generated
 at a certain isobaric level, which is 100 hPa (Dmitrieva et al., 2013). The height H of this level
 depends on the atmospheric temperature. The deviation of the count rate of the installation,
 110 therefore, depends on the change in the height of the generation level ΔH and the change in the
 temperature of this layer of air:

$$\left(\frac{\Delta N}{N_0}\right)_T = \alpha_H \Delta H + \alpha_T \Delta T \quad (3)$$

where

$\left(\frac{\Delta N}{N_0}\right)_T$ – count rate relative variations of the CARPET installation;

ΔH – absolute deviation of the effective generation level [km];

115 α_H – negative temperature coefficient [%/km];

ΔT – absolute temperature deviation at the level of effective generation [°C];

α_T – positive temperature coefficient [%/°C].

Upper-air meteorological sondes are launched twice a day, at 11:30 and 23:30 UTC. The picture
 of a typical MRZ-3AK1 sonde is presented in Fig. 5. Flights last, on average, about 1.5 hours,
 120 therefore, from the available data of the CARPET-MOSCOW installation were made samples of
 hourly data from 12:00 to 13:00 UTC and 00:00 to 01:00 UTC.

To calculate the contribution of the negative component of the temperature effect, we define the
 linear relationship between $\frac{\Delta N}{N_0}$ and ΔH (Fig. 6),

where

125 $\Delta N = N_{PC} - N_0$;



$$\Delta H = H - H_0;$$

H_0 – average (standard) height of the level of effective generation [km] for 2019–2020;

H – current height of the level of effective generation [km].

For the CARPET-MOSCOW installation: $H_0 = 16.1$ km, $\sigma_H = 0.3$ km. Using the least squares
 130 method, we define the approximating line, the slope of which is equal to α_H .

$\alpha_H = -4.00684 \pm 0.0652\%/km$; coefficient of determination $R^2 = 0.8191$.

Corrected data series (Fig. 4c) is calculated by the equation:

$$N_{HPC} = N_{PC} - \alpha_H N_0 \Delta H, \quad (4)$$

where

N_{HPC} – count rate [pulses/h] of the CARPET installation with negative temperature effect
 135 correction.

To calculate the contribution of the positive component of the temperature effect, we define the
 linear dependence between $\frac{\Delta N}{N_0}$ and ΔT (Fig. 7),

where

$$\Delta N = N_{HPC} - N_0;$$

$$140 \quad \Delta T = T - T_0;$$

T_0 – average (standard) temperature at the level of effective generation [°C] for 2019–2020
 according to CAO measurements;

T – current temperature at the level of effective generation [°C].

$T_0 = -56.9$ °C, $\sigma_T = 6.0$ °C.

145 Using the least squares method, we define the approximating line, which slope is α_T .

$\alpha_T = 0.0080 \pm 0.0038\%/^{\circ}C$; coefficient of determination $R^2 = 0.0049$.

As seen in Fig. 7, there is a slight positive temperature effect. Corrected data series is calculated
 by the equation (Fig. 4d):

$$N_{THPC} = N_{HPC} - \alpha_T N_0 \Delta T, \quad (5)$$

where

150 N_{THPC} – count rate [pulses/h] of the CARPET installation with positive temperature effect
 correction.

2.2.2 Integral method

Consider the integral method for determining the temperature effect:

$$\left(\frac{\Delta N}{N_0} \right)_T = \int_0^P \alpha(x) \Delta T(x) dx \quad (6)$$

where



155 P – atmospheric pressure at the point of determination of the temperature effect;

$\alpha(x)$ – temperature coefficient density;

$\Delta T(x)$ – temperature deviation from the average value in the air layer corresponding to the pressure from x to $x+dx$.

There are 16 isobaric surfaces commonly accepted while analyzing upper-air atmospheric effects:
 160 1000, 925, 850, 700, 500, 400, 300, 250, 200, 150, 100, 70, 50, 30, 20, and 10 hPa. They are also used in observations by CAO. It was decided to exclude the surface of 10 hPa from the calculations, since for the time period 2019 - 2020 there are only 148 measurements for this isobaric surface pressure level.

Represent equation 6 as a sum:

$$\left(\frac{\Delta N}{N_0}\right)_T = \sum_P \alpha(P) \Delta T(P) \quad (7)$$

165 where

$\alpha(P)$ – temperature coefficient for a given isobaric surface [%/°C];

$\Delta T(P)$ – deviation of temperature from the average value for a given isobaric surface [°C].

Starting from the first isobaric surface (20 hPa), we will determine the dependence between $\frac{\Delta N}{N}$ and ΔT . The corrected data for the first surface is then used to determine the temperature
 170 coefficient for the next surface, and so on:

$$N_{i+1} = N_i(1 - \alpha_{i+1} \Delta T_{i+1}), \quad (7)$$

where

$\alpha(P)$ – temperature coefficient of the isobaric surface $i+1$ [%/°C];

$\Delta T(P)$ – temperature deviation from the average value for the isobaric surface $i+1$ [°C];

N_i – count rate of the CARPET-MOSCOW, with temperature correction along the isobaric surface
 175 i ;

N_{i+1} – count rate of the CARPET-MOSCOW, with temperature correction along the isobaric surface $i+1$;

The results are shown in Table 1: the first column is the atmospheric pressure on the given surface, the second column is the average temperature according to the data for 2019 - 2020, the third
 180 column is the standard deviation of the temperature, the fourth column is the temperature



coefficient for the given isobaric surface, the fifth column is number of measurements. In fig. 4e shown the count rate of the CARPET-MOSCOW installation, corrected with integral method, according to the data for 2019 - 2020.

3. Conclusion

185 This paper describes the CARPET installation, designed for detecting the charged component of secondary CRs. The barometric coefficient was determined using the built-in pressure sensor. The temperature coefficient was determined by two methods using the data of the upper-air sounding. The results obtained by the effective generation method and the integral method correlate with each other. In this connection, it is more optimal to use the method of the effective generation
 190 level, since it does not require a complete temperature profile. Also, for the CARPET-MOSCOW installation, it is possible to use only the negative component of the temperature effect, since variations of the count rate have good ($R^2 = 0.8191$) correlation with ΔH .

Data availability. Data related to this article are available upon request to the corresponding authors.

195 *CRedit author statement*

M. Philippov: Conceptualization, Methodology, Software, Electronics, Data curation, Writing- Original draft preparation,

V. Makhmutov: Conceptualization, Methodology, Data curation, Writing- Original draft preparation,

200 **G. Bazilevskaya:** Conceptualization, Writing- Original draft preparation,

F. Zagumennov: Data curation, Original draft preparation,

V. Fomenko: Data curation,

Yu. Stozhkov: Conceptualization,

A. Orlov: Data curation.

205 4. Acknowledgments

The authors express their gratitude to the Neutron Monitor Database (NMDB) team (www01.nmdb.eu) for the data from the ground network of neutron monitors.



References

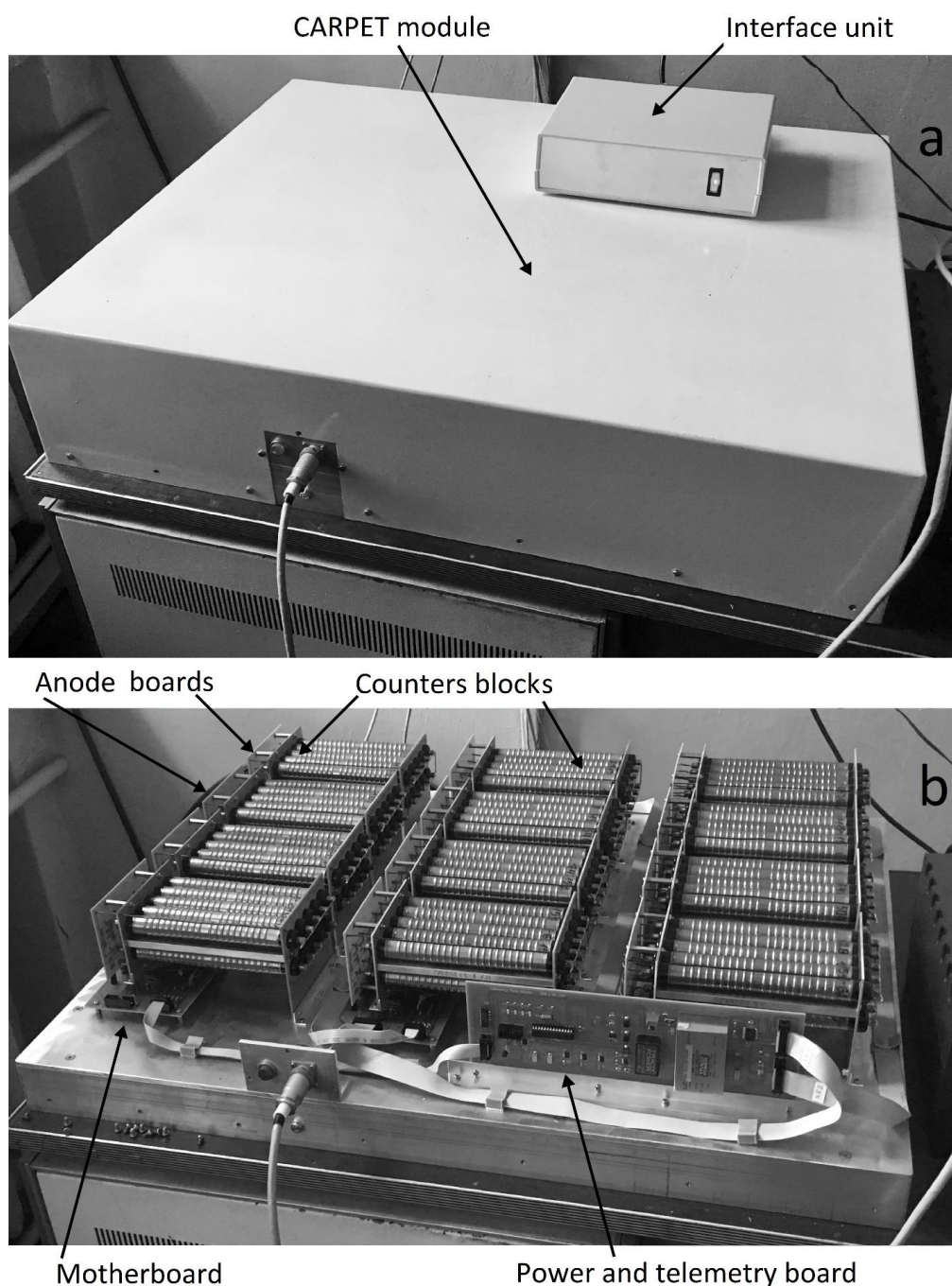
- 210 De Mendonca R., Raulin J.-P., Bertoni F., Echer E., Makhmutov V., and Fernandes G.: Long-term and transient time variation of cosmic ray fluxes detected in Argentina by CARPET cosmic ray detector. *JASTP*, 73, 410, doi: 10.1016/j.jastp.2010.09.034, 2011.
- De Mendonca R.R.S., Raulin J.-P., Echer E., Makhmutov V.S., and Fernandez G.: Analysis of atmospheric pressure and temperature effects on cosmic ray measurements, *J. Geophys. Res.: Space Phys.*, 118(4), 1403-1409, doi: 10.1029/2012JA018026, 2013.
- 215 Dmitrieva A. N., Astapov I. I., Kovylyayeva A. A., and Pankova D. V.: Temperature effect correction for muon flux at the Earth surface: estimation of the accuracy of different methods, *Journal of Physics: Conference Series*, 409, 012130, doi: 10.1088/1742-6596/409/1/012130, 2013.
- 220 Dorman, L. I.: *The Meteorological Effects of Cosmic Rays*, Nauka Press, Moscow, Russia, 1972.
- Dorman, L.: *Cosmic rays in the Earth's atmosphere and underground*, Kluwer Academic Publishers, USA, 2004.
- Dorman L.: Long-term cosmic ray intensity variation and part of global climate change, controlled by solar activity through cosmic rays, *Advances in Space Research.*, 37 (8), 1621-1628, doi: 10.1016/j.asr.2005.06.032, 2006.
- 225 Ganeva M., Peglow S., Hippler R., Berkova M., and Yanke V.: Seasonal variations of the muon flux seen by muon telescope MuSTAnG, *J. Phys. Conf. Ser.*, 409, 012242, 201.
- doi: 10.1088/1742-6596/409/1/012242, 2013.
- Maghrabi, A., Makhmutov, V.S., Almutairi, M., Aldosari, A., Altilasi, M., Philippov, M.V., and
- 230 Kalinin, E.V.: Cosmic ray observations by Carpet detector installed in central Saudi Arabia—preliminary results, *J. Atmos. Sol.-Terr. Phys.*, 200, 105194.
- doi: 10.1016/j.jastp.2020.1051942020, 2020.
- Makhmutov V., Raulin J.-P., De Mendonca R.R.S., Bazilevskaya G.A., Correia E., Kaufmann P., Marun A., Fernandes G., and Echer E.: Analysis of cosmic ray variations observed by the
- 235 CARPET in association with solar flares in 2011-2012. *J. Physics: Conf. Ser.*, 409(1), 012185/1-4, doi: 10.1088/1742-6596/409/1/012185, 2013.
- Makhmutov V. S., Bazilevskaya G. A., Stozhkov Y. I., Raulin J.-P., and Philippov M. V.: Analysis of Cosmic Ray Variations Recorded in October–December 2013, *Bulletin of the Russian Academy of Sciences. Physics*, 79(5), 570–572, doi: 10.3103/S1062873815050299,
- 240 2015.



- Mizin S.V., Makhmutov V.S., Maksumov O.S., and Kvashnin A.N.: Application of multithreading programming to physical experiment, *Kratk. Soobshch. Fiz.*, 2, 9 – 17, doi: 10.3103/S1068335611020023, 2011.
- Philippov, M.V., Makhmutov, V.S., Stozhkov, Y.I., and Maksumov O.S.: The CARPET Ground Facility for Detecting the Charged Component of Cosmic Rays, *Instrum Exp Tech*, 63, 388–395, doi: 10.1134/S0020441220030033, 2020a.
- Philippov M.V., Makhmutov V.S., Stozhkov Yu.I., Maksumov O.S., Bazilevskaya G.A., Morzabaev A.K., and Tulekov Ye. A.: Characteristics of the ground-based « CARPET-ASTANA » instrument for detecting charged component of cosmic rays and preliminary analysis of the first experimental data, *Nuclear Instruments and Methods in Physics Research Section A: Accelerators, Spectrometers, Detectors and Associated Equipment*, 959, 163567, doi: 10.1016/j.nima.2020.163567, 2020b.
- Tulekov, E.A., Makhmutov, V.S., Bazilevskaya, G. A., Stozhkov, Yu. I., Morzabaev, A. K., Philippov, M. V., Erkhov, V. I., and Dyusembekova, A. S.: Ground-based Instrument for the Study of Cosmic Ray Variation in Nur-Sultan, *Geomagn. Aeron.*, 60, 693–698, doi: 10.1134/S0016793220060134, 2020.
- Yanke V., Asipenka A., Berkova M., De Mendonca R.R.S., Raulin J.-P., Bertoni F.C.P., Echer E., Fernandez G., and Makhmutov V.: Temperature effect of general component seen by cosmic ray detectors, *Proceedings of 32nd International Cosmic Ray Conference*, 11, 377–380, doi: 10.7529/ICRC2011/V11/0627, 2011.
- Zazyan M., Ganeva M., Berkova M., Yanke V., and Hippler R.: Atmospheric effect corrections of MuSTAnG data, *J. Space Weather Space Clim.*, 5(A6), doi: 10.1051/swsc/2015007, 2015.

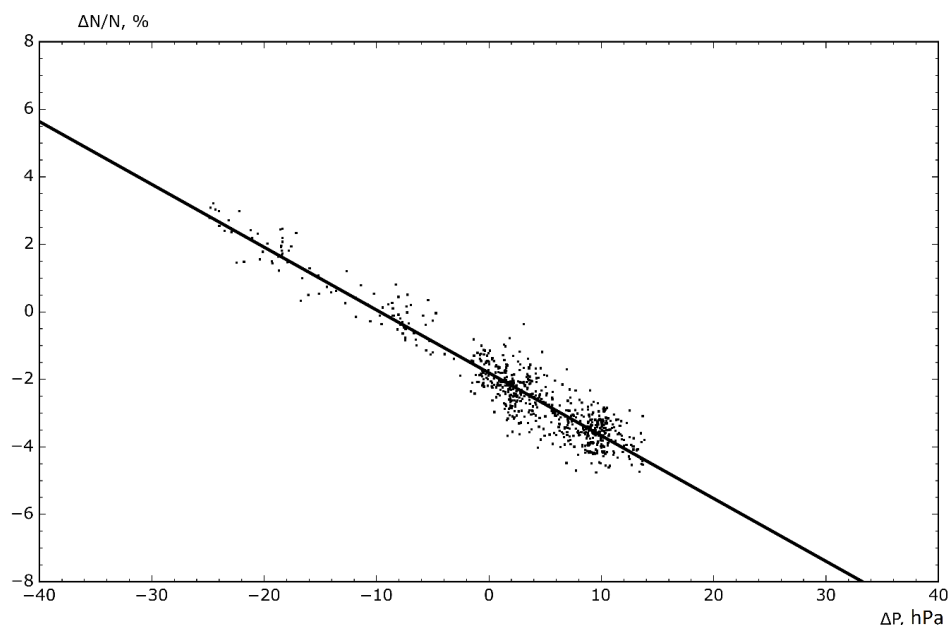


Figures

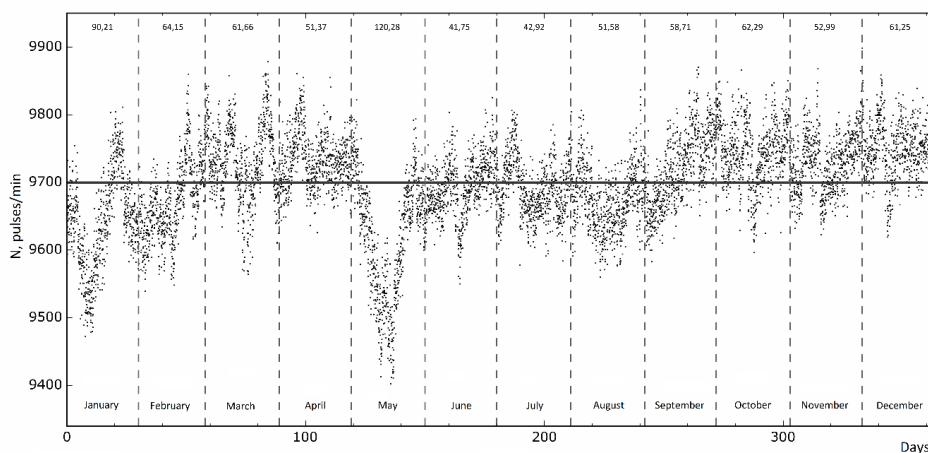


265

Fig. 1. CARPET-MOSCOW installation and its components. On panel *a* – CARPET module with cover and on panel *b* – CARPET module without cover.



270 **Fig. 2.** Relationship between $\frac{\Delta N}{N_0}$ and ΔP for the CARPET-MOSCOW installation determined on
 the data of June 2019



275 **Fig. 3.** Count rate variations of the Moscow neutron monitor for the period of 2019. Horizontal
 line – average count rate.

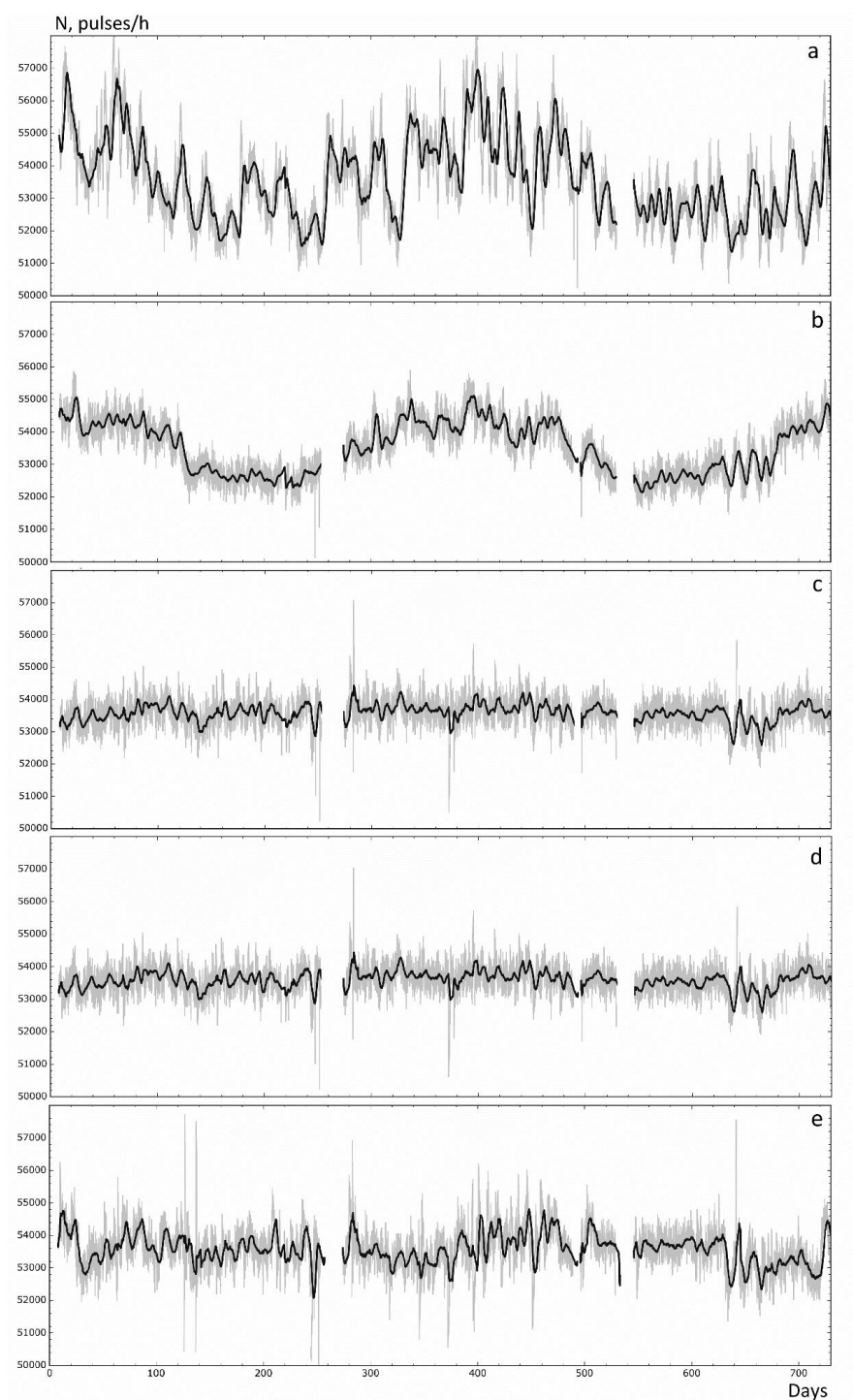


Fig. 4. Count rate variations of the CARPET-MOSCOW installation: *a* – uncorrected data, *b* – pressure corrected data, *c* - pressure and temperature (negative effect) corrected data, *d* – pressure



280 and temperature (negative and positive effect) corrected data, e – pressure and temperature
(integral method) corrected data.

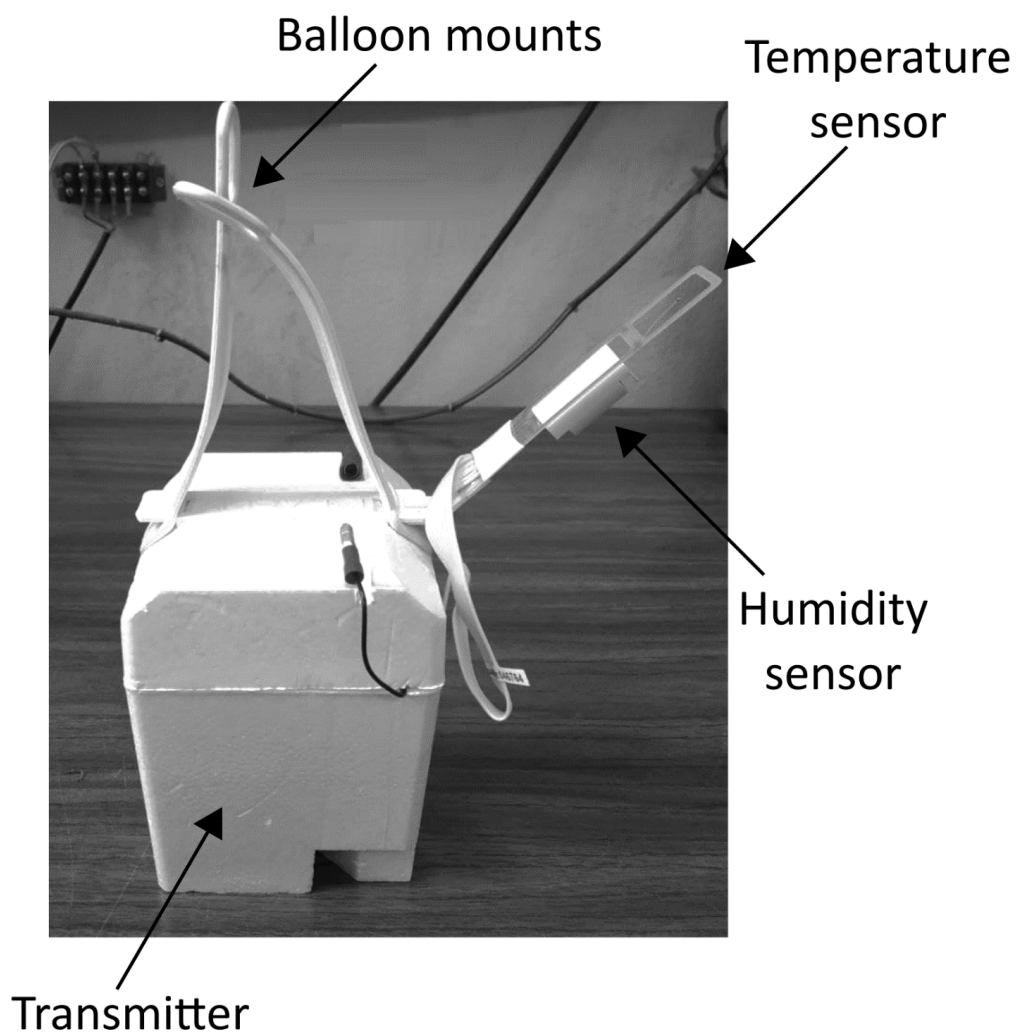
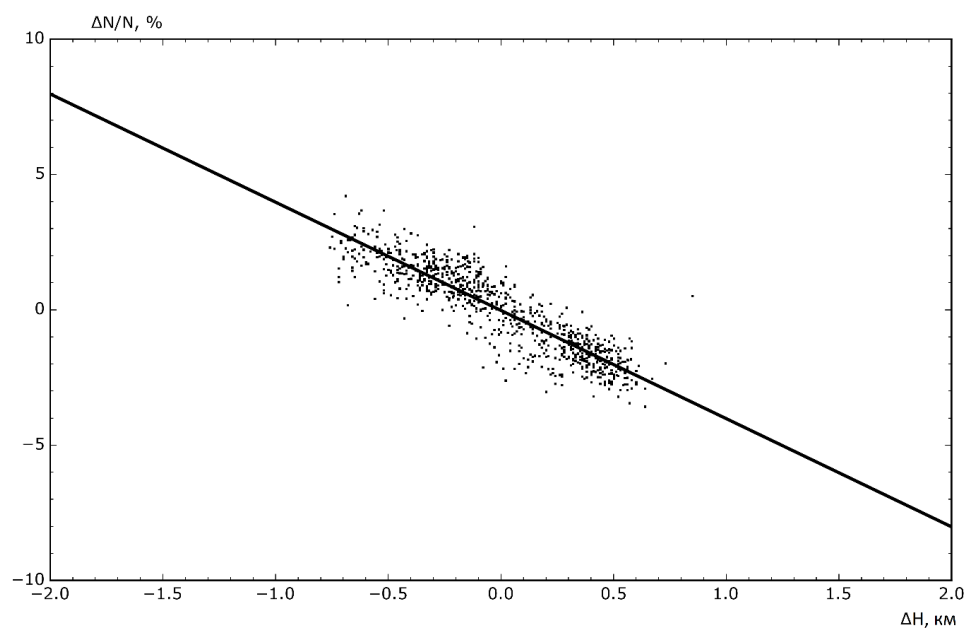


Fig. 5. Upper air sonde MRZ-3AK1 (CAO; Dolgoprudny)



285

Fig. 6. Relationship between $\frac{\Delta N}{N_0}$ and ΔH (negative temperature effect) for the CARPET-MOSCOW installation determined on the data of 2019-2020

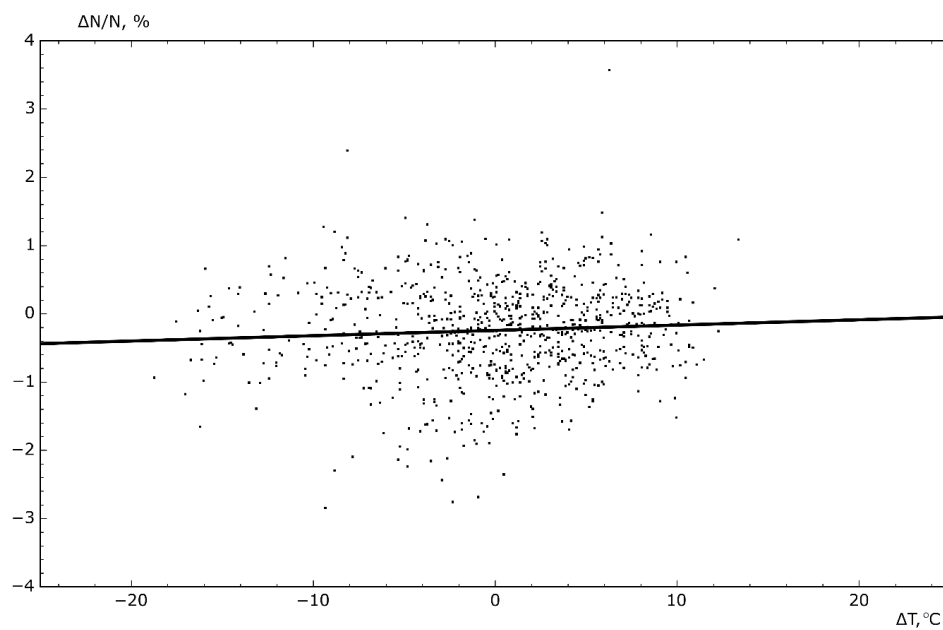


Fig. 7. Relationship between $\frac{\Delta N}{N_0}$ and ΔT (positive temperature effect) for the CARPET-MOSCOW

290 installation determined on the data of 2019-2020



Tables

P , hPa	\bar{T} , °C	σ_T , °C	α , %/°C	n
20	-57,13	11,30	-0,0909±0,0041	670
30	-59,00	9,04	-0,0193±0,0047	764
50	-59,09	7,45	-0,0078±0,0055	807
70	-58,30	6,46	0,0023±0,0015	826
100	-56,97	6,00	-0,0004±0,0067	859
150	-55,52	6,46	-0,0100±0,0068	849
200	-56,56	7,03	0,0094±0,0031	859
250	-54,03	5,57	-0,0580±0,0069	863
300	-47,63	5,91	-0,0657±0,0061	863
400	-33,62	7,11	-0,0366±0,0049	868
500	-22,22	7,45	-0,0078±0,0047	868
700	-6,79	7,30	-0,0071±0,0025	874
850	0,76	7,78	0,0086±0,0045	881
925	3,92	9,00	0,0161±0,0039	879
1000	2,62	8,71	0,0124±0,0098	170

295 **Table.1.** The results of determining the temperature coefficient for each isobaric surface.